# NUCLEON SINGLE-PARTICLE ENERGY LEVELS IN $^{51}$Fe AND $^{51}$Mn MIRROR NUCLEI

Aye Aye Min[1], Nang Khin Saw Aung[2] and Khin Swe Myint[3]

## Abstract

In this paper, both the neutron and proton single-particle energy levels of A=51 mirror nuclei, $^{51}$Fe and $^{51}$Mn have been investigated by solving non-relativistic Schrödinger equation within the framework of Numerov method. In this calculation, phenomenological Woods-Saxon potential with spin-orbit interaction has been applied. Coulomb interaction is also taken into account for proton single-particle model approach. We also found that proton single-particle energy levels are higher than the neutron single-particle energy levels due to the effect of Coulomb repulsion. Moreover, there is some energy discrepancy between $^{51}$Fe and $^{51}$Mn mirror nuclei for proton single-particle model. This is due to the fact that the number of protons and neutrons are interchanged in the mirror nuclei. Moreover, the total root-mean-square radii of these mirror nuclei have also been investigated and the calculated values are found to be 3.57 fm for $^{51}$Fe and 3.56 fm for $^{51}$Mn respectively. We also observed the peculiar behavior in the relation between the binding energies and root-mean-square radii. Furthermore, the one nucleon and two nucleons separation energies have been investigated.

**Keywords**: mirror nuclei, single-particle energy levels, Numerov method

## Introduction

Investigation of the structure and energy levels of nuclei is the basic understanding of nuclear properties and nucleon-nucleon interaction. Thus, many nuclear models such as Fermi gas model, liquid drop model, single-particle shell model and cluster model have been introduced to develop the better understanding of the nuclear properties. Among nuclear models, single-particle shell model is one of the most fruitful model in order to probe the nuclear properties (Bakhshabadi, F. and S. Mohammadi,, (2015), Giv, B.N. and S. Mohammadi, (2017)). Nowadays, the study of mirror nuclei (Machleidt, R. and H. Muther, (2001)) is an interesting issue to understand the charge symmetry breaking effect. The mirror nuclei have the same nucleon numbers and therefore they should have identical nuclear interaction due to properties of nuclear force. But the symmetry is being mainly broken due to spin orientation and the effect of Coulomb interaction. The study of this symmetry breaking reveals the details of structure of the mirror nuclei. In this paper, the nucleon single-particle energy of A=51 mirror nuclei, $^{51}$Fe and $^{51}$Mn, was investigated within the shell model approach.

## Mathematical Formulation

### (a) Numerov Method for Numerical Calculation

In this research work, the neutron and proton single-particle energies of A=51 mirror nuclei have been studied within the framework of shell model approach. To investigate the nucleon single-particle energy level, one-body Schrödinger radial equation will be used.

[1] Dr, Associate Professor, Department of Natural Science, University of Computer Studies (Magway)
[2] Master of Research Student, Department of Physics, University of Mandalay
[3] Rector (Rtd.), University of Mandalay

$$\frac{d^2u(r)}{dr^2} + k(r)\,u(r) = 0 \text{ or } u''(r) = -k(r)\,u(r), \text{ where } k(r) \equiv \frac{2M}{\hbar^2}\left[E - V(r) - \frac{\hbar^2}{2M}\frac{\ell(\ell+1)}{r^2}\right] \quad (1)$$

In this equation, k(r) is the kernel of the equation, M is the mass of nucleon single-particle, and V(r) is the potential of the single nucleon in the field of remaining core nucleus and u (r) is the reduced radial wave function. Equation (1) can be solved by means of Numerov method. In this method, the r range (r) is split into N points according to $r_n = r_{n-1} + h$ where h is the step and then the wave function and kernel of the equation can be rewritten as $u_n \equiv u(r_n) = u(r_{n-1} + h)$ and $k_n \equiv k(r_n) = k(r_{n-1} + h)$. Then, we can expand $u(r)$ by using Taylor series,

$$u_{n+1} \equiv u(r_n + h) = u(r_n) + hu'(r_n) + \frac{h^2}{2}u''(r_n) + \frac{h^3}{6}u'''(r_n) + \frac{h^4}{24}u^{iv}(r_n) + 0(h^5) \quad (2)$$

$$u_{n-1} \equiv u(r_n - h) = u(r_n) - hu'(r_n) + \frac{h^2}{2}u''(r_n) - \frac{h^3}{6}u'''(r_n) + \frac{h^4}{24}u^{iv}(r_n) + 0(h^5) \quad (3)$$

By adding equations (2) and (3), we obtain

$$u(r_n + h) = 2\,u(r_n) - u(r_n - h) - h^2\,k(r_n)\,u(r_n) + \frac{h^4}{12}u^{iv}(r_n) \quad (4)$$

Similarly, the second-order derivative of the wave function can also be written as

$$u''_{n+1} \equiv u''(r_n + h) = u''(r_n) + hu'''(r_n) + \frac{h^2}{2}u^{iv}(r_n) + \frac{h^3}{6}u^{v}(r_n) + 0(h^6) \quad (5)$$

$$u''_{n-1} \equiv u''(r_n - h) = u''(r_n) - hu'''(r_n) + \frac{h^2}{2}u^{iv}(r_n) - \frac{h^3}{6}u^{v}(r_n) + 0(h^6) \quad (6)$$

As the same procedure of equation (2) and (3), the following equation can be obtained.

$$h^2u^{iv}(r_n) = -k(r_{n+1})\,u(r_{n+1}) - k(r_{n-1})\,u(r_{n-1}) + 2k(r_n)\,u(r_n) \quad (7)$$

By substituting equation (7) into equation (4) and solving, we get the following equations.

$$u_n = \frac{2\left[1 - \frac{5h^2}{12}k_{n-1}\right]u_{n-1} - \left[1 + \frac{h^2}{12}k_{n-2}\right]u_{n-2}}{\left[1 + \frac{h^2}{12}k_n\right]} \quad (8)$$

$$u_{n-1} = \frac{2\left[1 - \frac{5h^2}{12}k_n\right]u_n - \left[1 + \frac{h^2}{12}k_{n+1}\right]u_{n+1}}{\left[1 + \frac{h^2}{12}k_{n-1}\right]} \quad (9)$$

The above two equations are the forward and backward recursive relations in order to find the wave function for our consideration system. Therefore, when we calculate the wave function by using the forward-backward technique, it is necessary to give two initial values for each

direction and the two solutions at the origin and the asymptotic solution at $r \to \infty$ are $u(r \to 0) = r^{-\ell}$ and $u(r \to \infty) = e^{-\alpha r^2}$, $\alpha$ = constant. The first derivative wave function is

$$u'_n = \frac{1}{2h}\left[\left(1+\frac{h^2}{6}k_{n+1}\right)u_{n+1} - \left(1+\frac{h^2}{6}k_{n-1}\right)u_{n-1}\right] \tag{10}$$

Since both $u_{out}(r)$ and $u_{in}(r)$ satisfy in a homogeneous equation, their normalization can always be chosen so that they are set to be equal at the $r_c$ point. At the matching point $r_c$ the eigen functions must all satisfy the continuity conditions as the following.

$$(u_{out})_{r_c} = (u_{in})_{r_c},\ (u'_{out})_{r_c} = (u'_{in})_{r_c} \tag{11}$$

We can define a G(E ) function at $r_c$ whose zeros correspond to the energy eigenvalues as;

$$G(E) = \left[\frac{u'_{out}}{u_{out}}\right]_{r_c} - \left[\frac{u'_{in}}{u_{in}}\right]_{r_c}. \tag{12}$$

Firstly, we give a trial energy "E" as an input at r = 0 and this energy is increased according to the equation $E_n = E + \Delta E$ where $\Delta E$ is the energy step within the N points. For each $E_n$, their eigen functions $u_{out}$ and $u_{in}$ can be calculated at the $r_c$ point and build the G(E ) function. We carefully looked for and checked a change of sign in the value of G(E ) function. When we find it, we perform a fine tuning closing the energy range until the required tolerance. The correct energy eigen value and corresponding eigen function can be obtained simultaneously if the value of G(E) function is zero or very close to zero. In this calculation, we choose that the matching point is N/3.

**(b) Derivation of Normalized Wave function**

The outwards and inwards functions is directly obtained from the recursive formulas as $u_{out}(r)$ and $u_{in}(r)$ respectively.

The physical eigen functions $u_{out}(r)$ and $u_{in}(r)$ can be rewritten as

$$u_{out}(r) = A\,\Phi(r),\ u_{in}(r) = B\,I(r) \tag{13}$$

where A and B are constant. Their respective derivatives are

$$u'_{out}(r) = A\,\Phi'(r),\ u'_{in}(r) = B\,I'(r) \tag{14}$$

By substituting equation (13) and (14) in equation (11) respectively, we obtain as

$$(A\Phi)_{r_c} = (BI)_{r_c} \text{ and } (A\Phi')_{r_c} = (BI')_{r_c} \tag{15}$$

and performing the difference of the above equations, we get $A = \left[\frac{I - I'}{\Phi - \Phi'}\right]_{r_c} B \equiv f_c B$, where $f_c$ = scaling factor. Therefore, the above equation is the relation between the constant A and B. We have already got outwards ( $\Phi$ ) and inwards functions (I) from the recursive formulas. After

obtaining their derivatives, we can find the value of constant A. The value of constant B can be acquired after getting the value of A. Therefore, equation (14) can be rewritten as $u_{out}(r) = f_c B\ \Phi(r)$, $u_{in}(r) = B\ I(r)$, and B is the global factor that must be taken into account in the normalization process. Moreover, normalized constant "B" can be obtained by using the normalization conditions: $\int_0^{r_{max}} |u_\ell(r)|^2 dr = \int_0^{r_c} |u_{out}(r)|^2 dr + \int_{r_c}^{r_{max}} |u_{in}(r)|^2 dr = 1$. The global factor "B" is as $B = \frac{1}{\sqrt{N}}$, where, $N = \left[ f_c^2 \int_0^{r_c} |\Phi(r)|^2 dr + \int_{r_c}^{r_{max}} |I(r)|^2 dr \right]$. Therefore, the normalized eigen functions becomes, $u_{out}(r) = \frac{1}{\sqrt{N}} f_c\ \Phi(r)$ from r = 0 fm to $r_c$ point and $u_{in}(r) = \frac{1}{\sqrt{N}} I(r)$ from r = $r_c$ fm to $r_N$ point. The above wave functions are the normalized forward and backward wave functions in order to investigate the properties of nucleon single-particle states.

## Potential for Nucleon Single-particle

In order to calculate nucleon single-particle energy levels, we considered that the nucleon moves freely in an average potential well generated by the other nucleons. The phenomenological Woods-Saxon central potential including spin-orbit interaction (Min, A.A. et al., (2014)) was applied in this calculation. Therefore, Woods-Saxon potential including spin-orbit term for $j = \ell + \frac{1}{2}$ state and $j = \ell - \frac{1}{2}$ state are:

$$V(r) = \frac{-V_0}{1+e^{(r-R)/a}} - V_{so}\left(\frac{\hbar}{m_\pi c}\right)^2 \left(\frac{1}{2}\ell\right)\frac{1}{ra}\frac{e^{\frac{(r-R)}{a}}}{\left(1+e^{\frac{(r-R)}{a}}\right)^2} \tag{16}$$

$$V(r) = \frac{-V_0}{1+e^{(r-R)/a}} + V_{so}\left(\frac{\hbar}{m_\pi c}\right)^2 \left(\frac{1}{2}(\ell+1)\right)\frac{1}{ra}\frac{e^{\frac{(r-R)}{a}}}{\left(1+e^{\frac{(r-R)}{a}}\right)^2}. \tag{17}$$

The above two potentials can be used in order to calculate nucleon single- particle energy levels for each orbital angular momentum states of our consideration system. The value of $V_0$, $V_{so}$ and a are described in reference. It is also necessary to consider the Coulomb potential for the proton single-particle state. Since the core nuclei are not the point charged particles, the finite size Coulomb potential will, therefore, be used. Coulomb potential can be divided into three regions (i) the potential at a point outside the nucleus (r > R), (ii) the potential at on the surface of the nucleus (r ≥ R) and (iii) the potential inside the nucleus (r < R). By applying Gauss's theorem, we can derive Coulomb's potential for each region as $V_{Coulomb}(r) = Z_1 Z_2 \alpha \hbar c \frac{1}{r}$ (for $r \geq R$) and $V_{Coulomb}(r) = Z_1 Z_2 \alpha \hbar c \frac{1}{2R}\left[3 - \frac{r^2}{R^2}\right]$ (for $r < R$),

where $Z_1$ and $Z_2$ are charge of the single proton and core nucleus, $\alpha$ is the fine structure constant.

## Calculation of Root-mean-square Radii and Nucleon Separation Energies

After getting the normalized wave function, we can calculate the root-mean-square radii of mirror nuclei, $^{51}$Fe and $^{51}$Mn. The root-mean-square radius of the nucleon single-particle in each state can be obtained as $\langle r^2 \rangle = \langle u(r) | r^2 | u(r) \rangle$. In this equation, u(r) is the wave function of the corresponding states. The total root-mean-square radii of A=51 mirror nuclei (Rmst) can be deduced by using the following equation as $\text{Rmst} = \sqrt{\left(\frac{x_1}{x_2}\right)}$, where, $x_1 = \sum_i (2j_i + 1) \langle r^2 \rangle_i$ and $x_2 = \sum_i (2j_i + 1)$. The one-neutron and one-proton separation energies can be expressed as $S_n = B(Z, N) - B(Z, N-1)$ and $S_p = B(Z, N) - B(Z-1, N)$.

Based on the above equations, two-neutron separation energy and two-proton separation energy are $S_{2n} = B(Z, N) - B(Z, N-2)$ and $S_{2p} = B(Z, N) - B(Z-2, N)$. By using the above equations, one nucleon and two nucleon separation energies can be calculated.

## Results and Discussions

In this paper, the nucleon single-particle energy levels of A=51 mirror nuclei, $^{51}$Fe and $^{51}$Mn, have been investigated by using Woods-Saxon potential with spin-orbit interaction. In this calculation, Numerov method has been applied. The accuracy of this method has already checked by using harmonic oscillator potential model for $^{12}$C. The calculated numerical results are in good agreement with the analytical results. As a first step, the single-nucleon potentials have been analyzed. Fig. 1 (a) is the total potential of nucleon single-particle having the various spin-orbit coupling states in the nuclear medium. We found that the interaction range is about 8.0 fm for Woods-Saxon prescription. Moreover, the nucleon single particle field strongly depends upon the spin-orbit coupling. Therefore, the spin-orbit interaction for various orbital angular momenta have been plotted in order to recognize the behavior of this interaction and it is shown in Fig. 1 (b). From our graph, we can clearly see that the spin orbit potential for the Jackknife case gives the attractive interaction while that of the stretched spin case provides the repulsive interaction. In addition, there is no attractive or repulsive interaction in the nuclear interior but the spin-orbit potential is peaked near the nuclear surface.

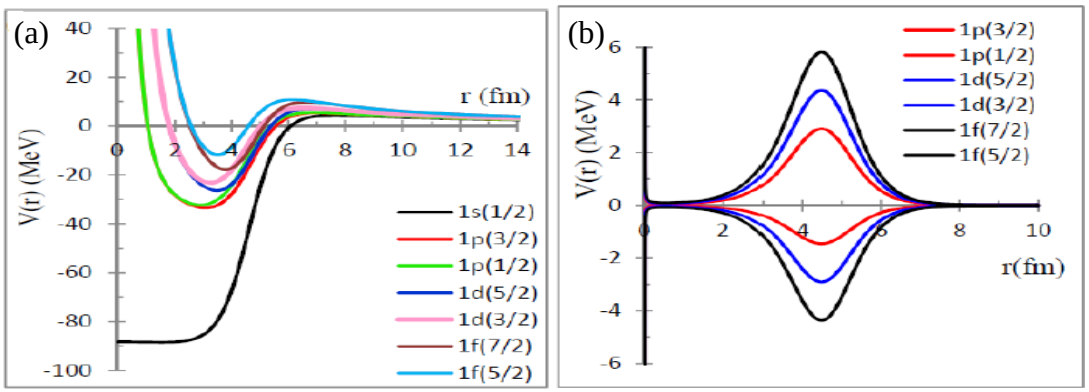


**Figure 1 (a)** Nucleon single-particle potential in the nuclear medium and (b) spin-orbit interaction for each state

The systematic energy level diagrams for neutron and proton single-particle energy levels in A= 51 mirror nuclei, $^{51}$Fe and $^{51}$Mn, are also displayed in Fig. 2 (a) and (b) respectively.

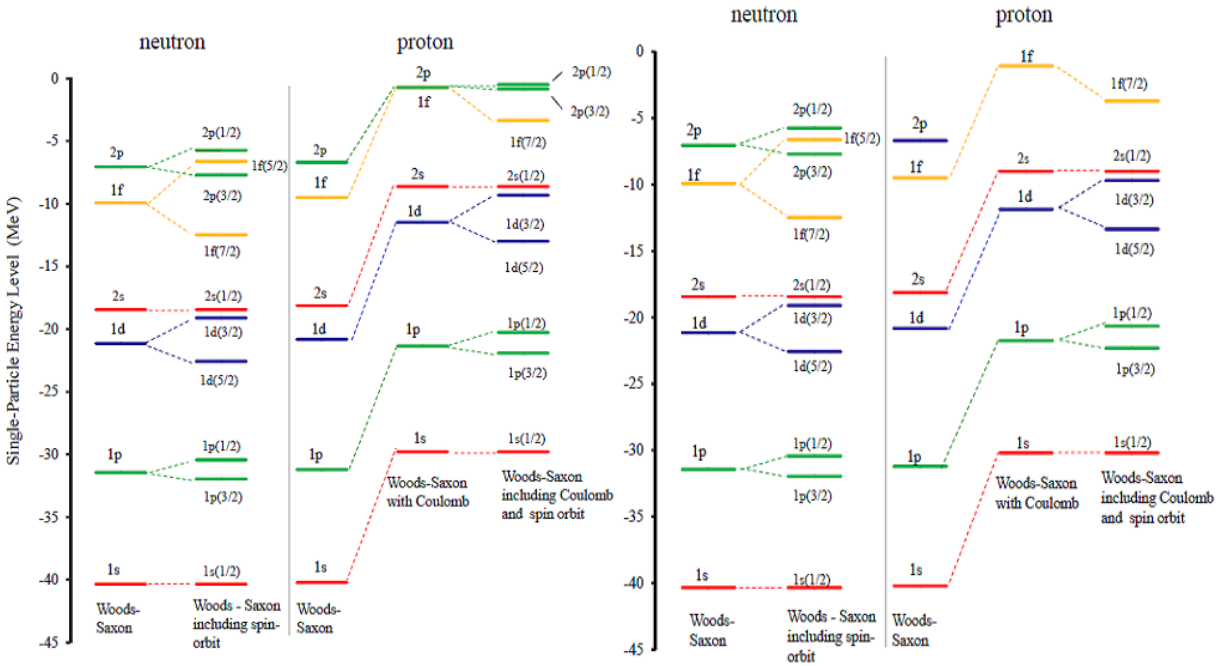


**Figure 2** Single-particle energy level (a) in $^{51}$ Fe (b) $^{51}$Mn

The neutron single-particle energy levels are the same for A= 51 mirror nuclei. However, proton single-particle energy levels are higher than the neutron single-particle energy levels due to the effect of Coulomb repulsive interaction between proton and core nuclei. Moreover, we can also see that proton single-particle energy levels have some energy discrepancy between $^{51}$Fe and $^{51}$Mn mirror nuclei. This is due to the fact that the number of protons and neutrons are interchanged in the mirror nuclei. In order to understand the difference in energy level qualitatively, we plotted it which is also called the Coulomb energy difference in $^{51}$Fe and $^{51}$Mn mirror nuclei. Fig. 3 (a) and (b) show the energy difference between neutron and proton single-particle model and the Coulomb energy difference in the mass number A= 51 mirror nuclei.

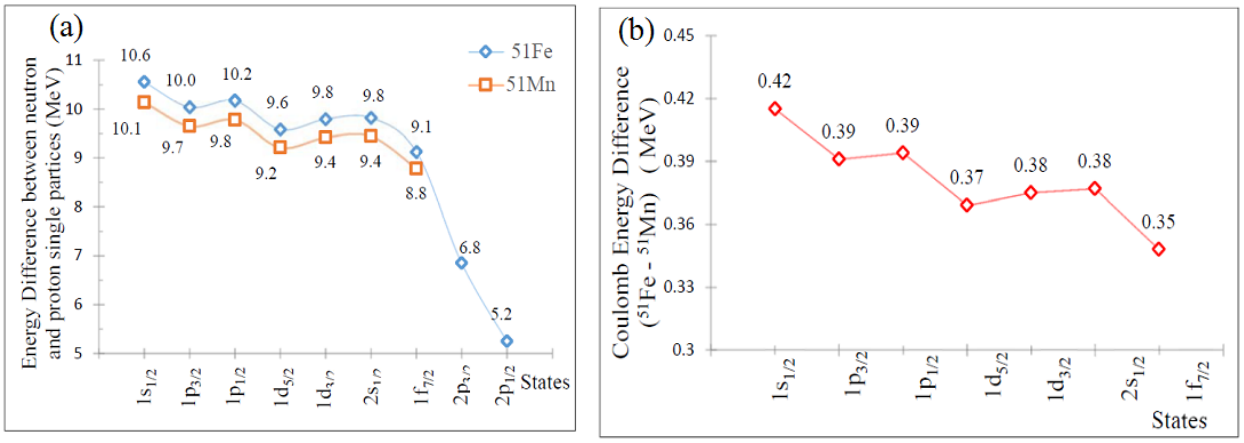


**Figure 3 (a)** Energy difference between neutron and proton single-particle model (b) Coulomb energy difference in A= 51 mirror nuclei.

The root-mean-square radii of A=51 mirror nuclei have also investigated for various nucleon single-particle states and the results are expressed in Tables (1) and (2).

**Table 1 Neutron single-particle energy levels of A=51 mirror nuclei**

| Single-particle state | Single-particle energy (MeV) (Woods-Saxon pot. only) | rms distance (fm) | Single-particle state | Single-particle energy (MeV) (Woods-Saxon pot.+ LS pot.) | rms distance (fm) |
|---|---|---|---|---|---|
| 1s | -40.34 | 2.63 | $1s_{1/2}$ | -40.34 | 2.63 |
| 1p | -31.44 | 3.17 | $1p_{3/2}$ | -31.96 | 3.20 |
| | | | $1p_{1/2}$ | -30.43 | 3.07 |
| 1d | -21.15 | 3.59 | $1d_{5/2}$ | -22.57 | 3.64 |
| | | | $1d_{3/2}$ | -19.11 | 3.52 |
| 2s | -18.44 | 3.51 | $2s_{1/2}$ | -18.44 | 3.51 |
| 1f | -9.91 | 4.00 | $1f_{7/2}$ | -12.48 | 4.04 |
| | | | $1f_{5/2}$ | -6.61 | 3.96 |
| 2p | -7.04 | 4.20 | $2p_{3/2}$ | -7.69 | 4.16 |
| | | | $2p_{1/2}$ | -5.74 | 4.26 |

According to our calculated results, the root-mean-square radii gradually increased with decreasing energy values within the frame work of Woods-Saxon interaction and this interaction including Coulomb interaction. But, when the spin-orbit interaction is switched on, we observed the peculiar behavior in the relation between the binding energies and root-mean-square radii. In order to understand this strange behavior clearly, the potential and the corresponding wave function for $^{51}$Fe have been plotted for various states.

These plotted figures is described in Fig 4. (a) and (b). The attractive interaction strength which possesses the total spin $J = \ell + s$ is stronger than that having $J = \ell - s$. The stronger interaction strength gives the greater binding energy. Moreover, the spin-orbit attractive potential works near the nuclear surface.

**Table (2) Proton single-particle energy levels of $^{51}$Fe and $^{51}$Mn**

| Nuclide | states | Single-particle energy (MeV) (Woods-Saxon +Coulomb) | states | Single-particle energy (MeV) (Woods-Saxon +Coulomb + LS coupling) | rms distance (fm) | Total rms distance (fm) |
|---|---|---|---|---|---|---|
| $^{51}$Fe | 1s | -29.79 | $1s_{1/2}$ | -29.79 | 2.70 | 3.57 |
| | 1p | -21.35 | $1p_{3/2}$ | -21.92 | 3.27 | |
| | | | $1p_{1/2}$ | -20.26 | 3.18 | |
| | 1d | -11.48 | $1d_{5/2}$ | -12.99 | 3.71 | |
| | | | $1d_{3/2}$ | -9.31 | 3.60 | |
| | 2s | -8.62 | $2s_{1/2}$ | -8.62 | 3.53 | |
| | 1f | -0.71 | $1f_{7/2}$ | -3.35 | 4.14 | |
| | | | $1f_{5/2}$ | - | - | |
| | 2p | -0.73 | $2p_{3/2}$ | -0.85 | 4.56 | |
| | | | $2p_{1/2}$ | -0.49 | 4.73 | |
| $^{51}$Mn | 1s | -30.20 | $1s_{1/2}$ | -30.20 | 2.70 | 3.56 |
| | 1p | -21.74 | $1p_{3/2}$ | -22.31 | 3.26 | |
| | | | $1p_{1/2}$ | -20.65 | 3.17 | |
| | 1d | -11.85 | $1d_{5/2}$ | -13.35 | 3.71 | |
| | | | $1d_{3/2}$ | -9.69 | 3.60 | |
| | 2s | -8.99 | $2s_{1/2}$ | -8.99 | 3.49 | |
| | 1f | -1.06 | $1f_{7/2}$ | -3.70 | 4.13 | |
| | | | $1f_{5/2}$ | - | - | |
| | 2p | - | $2p_{3/2}$ | - | - | |
| | | | $2p_{1/2}$ | - | - | |

Furthermore, single-nucleon wave functions for J= $\ell$ + s are more shifted to the outer region than that having spin state $J = \ell - s$ and that is why the root-mean-square radius of nuclei for each spin state is larger although the binding energy is large. These effects could explain why both the rms value and binding energy are large. The total root-mean-square radius of A=51 mirror nuclei have been investigated. The calculated results are 3.57 fm for $^{51}$Fe and 3.56 fm respectively.

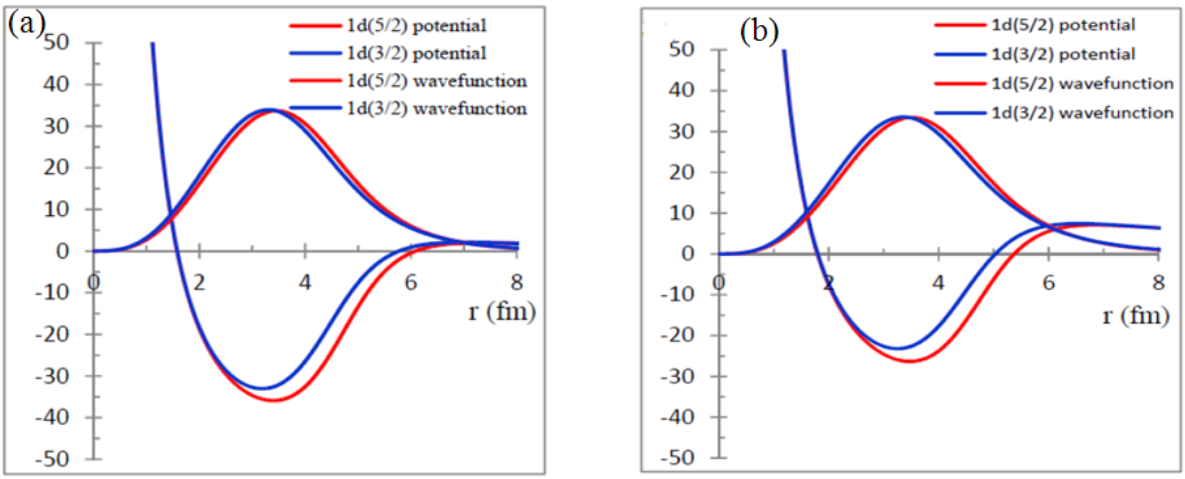


**Figure 4 (a)** Neutron and (b) proton single-particle wave functions and potentials for 1d state in $^{51}$Fe

Moreover, we have calculated one nucleon separation energies and two nucleon separation energies for A=51 mirror nuclei by using the binding energies data (Audi, G. et al., (2012)) and the results are shown in Table (3). According to our results, although mass numbers are the same for the mirror nuclei, the nucleon separation energies are not the same. We found that the proton separation energies for $^{51}$Fe are smaller than that for $^{51}$Mn but the neutron separation energies are conflict with the proton separation energies.

**Table 3 Nucleon separation energies for $^{51}$Fe and $^{51}$Mn**

| Nuclide | Neutron Separation Energy (MeV) | | Proton Separation Energy (MeV) | |
|---|---|---|---|---|
| | One-neutron SE | Two- neutron SE | One-proton SE | Two-proton SE |
| $^{51}$Fe | 13.83 | 31.65 | 4.91 | 9.50 |
| $^{51}$Mn | 13.69 | 26.75 | 5.27 | 14.86 |
| Difference | 0.14 | 4.90 | -0.36 | -5.36 |

For the neutron separation energy case, the difference energy values between $^{51}$Fe and $^{51}$Mn are 0.14 MeV and 4.90 MeV respectively for one-neutron and two-neutron separation energies. For proton separation energy case, the differences for one-proton and two-proton separation energies are found to be -0.36 MeV and -5.16 MeV correspondingly.

## Conclusion

In this research work, nucleon single-particle energy levels of A=51 mirror nuclei, namely $^{51}$Fe and $^{51}$Mn have been investigated by solving one-body Schrödinger equation with the use of phenomenological Woods-Saxon central potential including spin-orbit interaction. According to our results, the calculated shell structure of neutron single particle are the same for A= 51 mirror nuclei but that of proton single particle have some discrepancy. This shell structure and some energy difference in proton single-particle energy levels of $^{51}$Fe and $^{51}$Mn mirror nuclei comes from the different number of protons in the mirror nuclei although the mass numbers are the same. In order to understand the difference in energy level, the Coulomb energy differences have been investigated qualitatively. We can conclude that the larger the value of the orbital angular momentum, the smaller Coulomb energy difference is. For the same orbital angular momenta case, the Coulomb energy difference for stretched spin state is greater than that for jackknife state. In addition, nucleon separation energies have been investigated. This present work is not only to understand the nuclear shell structure but also to recognize how to apply the simple and good numerical Numerov's method.

## Acknowledgements

The authors would like to thank Dr Soe Lin Aung, Rector, University of Computer Studies (Magway), for his encouragement and to acknowledge Professor Dr. Y. Akaishi, KEK, Japan, for his valuable advice.

## References

Bakhshabadi, F. and S. Mohammadi, (2015) "Calculation of the Energy Levels of Phosphorus Isotopes (A=31 to 35) by Using OXBASH Code." Americ. J. Mod. Phys. 4(3-1), pp.15-22.

Giv, B.N. and S. Mohammadi, (2017) "Calculating Energy Levels in $^{49}$Mn/$^{49}$Cr Mirror Nuclei with OXBASH Code." SciencePG 5(5), pp.70-73.

Machleidt, R. and H. Muther, (2001) "Charge symmetry breaking of the nucleon-nucleon interaction: ρ-ω mixing versus nucleon mass splitting." Phys. Rev. C 63 034005, pp.1-10.

Min, A.A. et al., (2014) "Single-particle Energy Levels of $^{34}$Si, $^{35}$P and $^{36}$S." Univ. Res. J. **7**(4), pp.25-36.